



doi:10.1016/j.gca.2003.09.006

## Formation of Fe(III)-minerals by Fe(II)-oxidizing photoautotrophic bacteria

ANDREAS KAPPLER and DIANNE K. NEWMAN\*

California Institute of Technology, Pasadena, CA 91125, USA

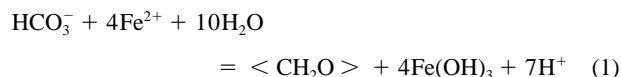
(Received June 5, 2003; accepted in revised form September 3, 2003)

**Abstract**—It has been suggested that Fe(II)-oxidizing photoautotrophic bacteria may have catalyzed the precipitation of an ancient class of sedimentary deposits known as Banded Iron Formations. In order to evaluate this claim, it is necessary to define and understand this process at a molecular level so that putative Fe-isotope “biosignatures” in ancient rocks can be interpreted. In this report, we characterize the substrates and products of photoautotrophic Fe(II)-oxidation by three phylogenetically distinct Fe(II)-oxidizing bacteria. In every case, dissolved Fe(II) is used as the substrate for oxidation, and there is no evidence for active dissolution of poorly soluble Fe(II)-minerals by biogenic organic ligands. Poorly crystalline Fe(III) (hydr)oxide mineral phases are initially precipitated, and as they age, rapidly convert to the crystalline minerals goethite and lepidocrocite. Although the precipitates appear to associate with the cell wall, they do not cover it entirely, and precipitate-free cells represent a significant portion of the population in aged cultures. Citrate is occasionally detected at nanomolar concentrations in all culture fluids, whereas an unknown organic molecule is always present in two out of the three bacterial cultures. Whether these molecules are released by the cell to bind Fe(III) and prevent the cell from encrustation by Fe(III) (hydr)oxides is uncertain, but seems unlikely if we assume Fe(II)-oxidation occurs at the cell surface. In light of the energetic requirement the cell would face to produce ligands for this purpose, and given the local acidity metabolically generated in the microenvironment surrounding Fe(II)-oxidizing cells, our results suggest that Fe(III) is released in a dissolved form as an inorganic aqueous complex and/or as a colloidal aggregate prior to mineral precipitation. The implication of these results for the interpretation of Fe-isotope fractionation measured for this class of bacteria (Croal et al., 2004) is that equilibrium processes involving free biological ligands do not account for the observed fractionation. Copyright © 2004 Elsevier Ltd

### 1. INTRODUCTION

Many different types of microorganisms can grow by oxidizing Fe(II). These include bacteria and archaea that couple Fe(II)-oxidation to the reduction of oxygen at either low (e.g., Blake et al., 1993; Edwards et al., 2000) or neutral pH (e.g., Emerson and Moyer, 1997); bacteria that couple Fe(II)-oxidation to the reduction of nitrate at neutral pH (e.g., Benz et al., 1998; Straub and Buchholz-Cleven, 1998); and bacteria that use Fe(II) as an electron donor in anoxygenic photosynthesis (e.g., Widdel et al., 1993; Ehrenreich and Widdel, 1994; Heising and Schink, 1998). These organisms can significantly affect the geochemistry of the Earth’s near surface environments. For example, acidophilic Fe(II) oxidizing bacteria and archaea play an important role in promoting acid mine drainage (Baker and Banfield, 2003), and neutrophilic Fe(II) oxidizing bacteria appear to contribute to the alteration of marine sediments (Edwards et al., 2003). From the perspective of early Earth history, however, arguably the most interesting types of Fe(II)-oxidizing bacteria are the anoxygenic photoautotrophs given that the evolution of Fe(II)-based photosynthesis likely preceded metabolisms based on oxygen or other highly oxidized species (i.e., nitrate).

As shown in Eqn. 1, modern-day photoautotrophic bacteria oxidize Fe(II) and use light energy for CO<sub>2</sub>-fixation (Widdel et al., 1993):



These bacteria are phylogenetically diverse, and include green sulfur bacteria (*Chlorobium ferrooxidans* strain KoFox; Heising et al., 1999), purple nonsulfur bacteria (e.g., *Rhodobacter ferrooxidans* strain SW2; Ehrenreich and Widdel, 1994) and purple sulfur bacteria (*Thiodictyon* sp. strain F4; Croal et al., 2004). Fe(II) can be used as an electron donor by anoxygenic phototrophs because the standard redox potential for Fe<sup>2+</sup>/Fe<sup>3+</sup> (+770 mV) is valid only at very acidic pH, whereas at neutral pH, the potential shifts to more negative values due to the low solubility of Fe(III). For example, the redox potential of the Fe<sup>2+</sup>/Fe<sup>3+</sup> couple for the bicarbonate-Fe(II)-Fe(III) system at neutral pH is approximately +200 mV, low enough to provide sufficient reducing power to sustain microbial growth (Widdel et al., 1993; Stumm and Morgan, 1996).

Photoautotrophic Fe(II)-oxidation has been proposed as a possible mechanism for the generation of massive sedimentary iron deposits known as Banded Iron Formations (BIFs) (Hartman, 1984; Widdel et al., 1993; Konhauser et al., 2002). BIFs formed throughout the early history of the Earth and are common in rocks older than 1.8 billion years. BIFs typically consist of alternating layers of chert and iron-bearing minerals (e.g., hematite, magnetite, siderite and pyrite; Beukes and Klein, 1992) and constitute the world’s major source of iron ore (Trendall and Morris, 1983). Despite intensive geologic investigation over the past century, these deposits remain one of the most enigmatic features in the geologic record, recording processes and conditions that apparently have been rare on Earth

\* Author to whom correspondence should be addressed (dkn@caltech.edu).

since the middle of the Proterozoic period, and absent since the late Precambrian (James and Sims, 1973; Beukes and Klein, 1992).

It has long been thought that these deposits were precipitated chemically from sea water when dissolved ferrous iron [Fe(II)] was oxidized to insoluble ferric iron [Fe(III)] by oxygen (O<sub>2</sub>) produced photosynthetically. However, because the most ancient BIFs (~3.8 Ga) formed during a period of Earth history when it is likely that O<sub>2</sub> was not present (Kasting, 1993), an anaerobic mechanism for Fe(II)-oxidation is required to explain their formation. Photochemical oxidation of Fe(II) (Cairns-Smith, 1978; Braterman et al., 1983; Francois, 1986) and photoautotrophic Fe(II)-oxidation are generally viewed as the most plausible alternatives, with more weight placed upon the latter (Konhauser, et al., 2002). In support of a role for Fe(II)-oxidizing photoautotrophs, Johnson et al. (2003) noted that the moderately positive  $\delta^{56}\text{Fe}$  values found in some oxide layers of the 2.5 Ga Kuruman and Griquatown Iron Formations might be explained by the enrichment of heavy iron atoms (<sup>56</sup>Fe) in the Fe(III) mineral products of photoautotrophic metabolism relative to the dissolved Fe(II) substrate (Croal et al., 2004).

Before we may conclude that the Fe isotope composition of Fe(III) minerals found in the most ancient BIFs reflect a "vital effect," however, we must understand the mechanisms of Fe isotope fractionation in both abiotic and biological systems. The Fe isotope fractionation produced by Fe(II)-oxidizing bacteria is comparable to that measured for dissimilatory Fe(III)-reducing bacteria (Beard et al., 1999) as well as to the fractionation measured for abiotic Fe(II)-oxidation by molecular oxygen followed by the rapid precipitation of ferrihydrite (Bullen et al., 2001). To reconcile these results, the Croal et al. (2004) study postulated two alternative mechanisms for the observed fractionations: 1.) that biologic ligands produce an equilibrium isotope effect, or 2.) that rapid precipitation of Fe(III) (hydr)oxide produces a kinetic isotope effect that overlies an equilibrium isotope effect produced by Fe(II)/Fe(III) ligand exchange. Because a detailed understanding of Fe transformation pathways is necessary to discriminate between these possibilities, we undertook the current study to define more precisely the steps involved in photoautotrophic Fe(II)-oxidation.

## 2. MATERIAL AND METHODS

### 2.1. Sources of Organisms

*R. ferrooxidans* strain SW2 was obtained from F. Widdel, MPI Bremen, Germany. *C. ferrooxidans* strain KoFox and *Thiodictyon* sp. strain F4 were obtained from B. Schink, University of Konstanz, Germany.

### 2.2. Media and Growth Conditions

All strains were cultivated in freshwater mineral medium prepared after Ehrenreich and Widdel (1994). The medium was buffered at pH 6.8 with bicarbonate. Vitamin and trace element solutions (1 mL each) and a vitamin B<sub>12</sub> solution (1 mL) were added (for details and concentrations see Ehrenreich and Widdel, 1994). This medium was used for growth with hydrogen (H<sub>2</sub>/CO<sub>2</sub>, v/v, 80/20) or acetate (10 mM). For experiments with different Fe(II) minerals, 25 mL of medium were transferred into 58-mL serum bottles containing the Fe(II) minerals (either 40 mM siderite, 20 mM vivianite, 20 mM pyrite, 20 mM magnetite or 40 mM ferrous sulfide). The bottles were closed with butyl rubber stoppers, crimped and the headspace was flushed with N<sub>2</sub>/CO<sub>2</sub>

(v/v, 80/20). The bottles were inoculated after 24 h of equilibration of the minerals in the medium.

For experiments with dissolved Fe(II), the medium was transferred into an anoxic glove-box and 10 mL of an anoxic 1 mol/L FeSO<sub>4</sub> stock solution was added followed by precipitation of a whitish-grey precipitate, probably consisting of vivianite and siderite formed by the Fe(II) added with the phosphate and bicarbonate present in the medium. After 24 h the medium was filtered (0.2 μm, cellulose nitrate, Millipore) leaving a clear solution with ~4–6 mM Fe(II). In uninoculated controls, no further precipitation was observed for the duration of the incubations. This method allowed us to analyze the Fe(III)-precipitates formed by the Fe(II)-oxidizing bacteria without Fe(II)-precipitates in the background. The medium (25 mL) was transferred into 58-mL serum bottles that were closed with butyl rubber stoppers, crimped and flushed with N<sub>2</sub>-CO<sub>2</sub> (v:v, 80:20). All cultures were incubated in the light. F4 and KoFox were incubated at 24°C; SW2 at 16–18°C.

For measurements of pH gradients with microelectrodes, *Rhodobacter ferrooxidans* strain SW2 colonies were grown in tubes with 1% agar as the solidifying agent. The agar (3.3 g) was washed three times with 200 mL water, suspended in 100 mL ultra pure water, autoclaved and dispensed in 3-mL aliquots into glass tubes. The tubes were kept at 60°C and 6 mL of the Fe(II)-containing medium was added and the tubes were transferred to a 40°C water bath. For the dilution series, 1 mL of culture suspension was added to the first tube. After gentle mixing, 1 mL was transferred to the next tube and the inoculated tubes were solidified in an ice-water bath. The tubes were flushed with N<sub>2</sub>-CO<sub>2</sub> (v:v, 80:20) and incubated under light at 16–18°C. Colonies developed after 3–4 weeks.

### 2.3. Iron Minerals

Vivianite and pyrite obtained as crystals from [www.mineralsunlimited.com](http://www.mineralsunlimited.com) (Minerals Unlimited, Ridgecrest, CA) were powdered in a mortar and identified by XRD. Siderite was a gift from M. Elsner, ETH/EAWAG Zürich, Switzerland. Magnetite and ferrous sulfide were purchased from Sigma-Aldrich. Ferrihydrite was prepared according to Schwertmann and Cornell (2000); its structure was confirmed by XRD analysis. Goethite was a gift from G. R. Rossman (Caltech).

The surface area of the minerals was determined by using the multipoint BET nitrogen adsorption technique (Micromeritics Gemini 2360 surface area analyzer) for siderite (117.3 m<sup>2</sup>/g), magnetite (6.8 m<sup>2</sup>/g), pyrite (2.4 m<sup>2</sup>/g), vivianite (3.1 m<sup>2</sup>/g), and ferrous sulfide (1.9 m<sup>2</sup>/g).

### 2.4. Analytical Methods

For analysis of dissolved iron, 200 μL culture suspension was withdrawn with a syringe, filtered in 0.5 mL Nylon (0.22 μm) filter tubes (Costar, Corning, NY) in an anoxic glove-box and analyzed for Fe(II) and Fe(III) with the ferrozine assay (Stookey, 1970). For analysis of total iron, 100 μL suspension was added to 900 μL 6 mol/L HCl and incubated for 1 h. After filtration with 0.22 μm Nylon filter tubes (Costar, Corning, NY), Fe(III) and Fe(II) were determined with the ferrozine assay.

pH microelectrodes (General Diamond, Ann Arbor, MI) with tip diameters of 2–10 μm were used to measure pH profiles around colonies grown in solidified agar tubes. The microelectrodes were mounted on a micromanipulator (General Diamond, Ann Arbor, MI) so that the electrode tip could be lowered into the agar in μm-increments.

The culture supernatants were analyzed for Fe(III)-siderophores with the CAS-assay after Schwyn and Neilands (1987) where in the presence of a strong Fe(III)-chelator, Fe(III) is removed from the blue ternary complex chrome azurol S/Fe(III)/hexadecyltrimethylammonium bromide and the color turns orange.

For analysis with ion chromatography (IC), high-pressure liquid chromatography (HPLC) and liquid-chromatography coupled to mass-spectrometry (LC-MS), culture supernatants were alkalinized with 10 mol/L NaOH (5 μL added to 1 mL supernatant), filtered in Nylon filter tubes (0.5 mL volume, 0.22 μm, Costar, Corning, NY) and concentrated by a factor of 10 under vacuum. HPLC- and LC-analysis were done with an Aminex HPX-87H column (Biorad) heated to 25°C. Either 30 mM phosphoric acid or 100 mM formic acid (0.6 mL/min)

were used as eluents in combination with a UV detector (absorbance followed at 210 and 254 nm) or a mass spectrometer, respectively. IC-analysis was done on an IonPac-column (ATC-I, Anion-Trap column, Dionex) with a flow-rate of 1 mL/min (0–2 min: 0.5 mM NaOH; 2.5–6 min: linear increase from 0.5 to 5 mM NaOH; 6–18 min linear increase from 5–38.25 mM NaOH) and a conductivity detector.

The equilibrium aqueous speciation in the medium was calculated with MINEQL (Environmental Research Software, Hallowell, ME).

## 2.5. Mineral Analyses

### 2.5.1. Powder X-ray diffraction

Samples of culture suspensions were withdrawn with a syringe in an anoxic glove-box and centrifuged to recover the precipitates. For analysis of 5-d old cultures, 4 mL of the culture suspension was centrifuged. From older cultures, 1 mL was sufficient for the analysis. To remove adsorbed Fe(II) from the precipitates (to avoid oxidation and formation of non-biogenic Fe(III)-precipitates) the biologically-produced precipitates were washed 2 times with ultra pure water that had been degassed under vacuum, flushed with N<sub>2</sub> and equilibrated under an anoxic atmosphere for several days. After spreading on a glass disk, the precipitates were dried in the glove-box. XRD spectra were obtained on a Scintag Pad V X-ray Powder Diffractometer using Cu-K $\alpha$  radiation operating at a 35 kV and 30 mA and a  $\theta$ - $2\theta$  goniometer equipped with a germanium solid-state detector. Each scan used a 0.04° step size from 10° to 80° with a counting time of 2 s per step. Structures were identified by comparison to spectra in the PCPDFWIN program, ©JCPDS-International Centre for Diffraction Data, 1997 (Newton Square, Pennsylvania) as well as to spectra of synthetic ferrihydrite and goethite.

To investigate Fe(III)-precipitates freshly formed by Fe(II)-oxidation and to avoid artifacts caused by old precipitates present from inoculating from 2-week-old cultures, different techniques were used: (i) cultures were inoculated from hydrogen-grown cultures (where no Fe(III)-precipitates were present) and (ii) only low amounts of inoculum from Fe(II)-grown cultures were used (1–5%). XRD-spectra of Fe(III)-precipitates obtained from these different cultures preparation techniques looked similar, leaving us confident that we were investigating the freshly formed precipitates.

### 2.5.2. Scanning electron microscopy (SEM)

Per sample, a 100  $\mu$ L culture suspension was withdrawn with a syringe and diluted in 300  $\mu$ L ultra pure water that had been degassed under vacuum, flushed with N<sub>2</sub>, and equilibrated under an anoxic atmosphere for several days. One drop of this suspension was spread on a carbon-coated copper grid (200 Mesh, 3 mm, SPI, West Chester, PA) and dried under an anoxic atmosphere in the glove-box. The samples were examined by a LEO 1550VP Field Emission SEM with an Oxford INCA energy dispersive X-ray spectroscopy. The system was operated at 1–15 kV for high resolution secondary electron imaging and elemental analysis. Because of reduced beam penetration, the low voltage SEM (<5kV) was particularly useful in surface imaging of the uncoated, fine particles.

### 2.5.3. Transmission electron microscopy (TEM)

Per sample, 5 mL of culture supernatants were centrifuged, fixed in 2.5–3% (v/v) glutaraldehyde at 4°C and washed 3 times in water. Half of the samples were stained with 2% osmium tetroxide and 2% uranyl acetate, while the other half were left unstained. Both stained and unstained specimens were then dehydrated in ethanol and acetone before embedding in EPON resin. After 24 h at 60°C samples were cut on a MT-X Ultramicrotome with a 55° Diatome diamond knife to a 60-nm thickness; ultrathin sections were placed on 200 mesh copper grids. The prestained samples were subsequently post-stained with 2% uranyl acetate for 3 min before final imaging. An Akashi EM-002B microscope operating at 100 kV was used for microscopy and EDS. The area sampled by the Oxford spectrum analyzer is approximately 8.8 nm at 83 kV. Acquisition rates were maintained at 10–20% dead time with 60 s live time. The electron beam was defocused at the condenser lens to maintain counting rates below 1 kHz and live time

efficiency >95%. The EDS patterns were recorded on an INCA 3.04 Microanalysis Suite and digitized for analysis.

## 3. RESULTS

### 3.1. Fe(II)-Oxidation by Photoautotrophic Bacteria

Three different strains of photoautotrophic Fe(II)-oxidizing bacteria, *Rhodobacter ferrooxidans* strain SW2, *Chlorobium ferrooxidans* strain KoFox and *Thiodictyon* sp. strain F4, were all able to oxidize 4–6 mM dissolved Fe(II) to completion within 2–3 weeks (Fig. 1) producing orange-brown Fe(III)-precipitates. Analysis of total iron after acid extraction showed that no Fe(II) was adsorbed to the Fe(III)-precipitates after complete oxidation of the dissolved Fe(II). Because most of the ferrous iron in nature is present in mineral form, we investigated whether and to what extent our strains could oxidize and/or actively dissolve various Fe(II)-minerals with different solubilities (Table 1). All three strains were able to oxidize siderite (FeCO<sub>3</sub>) and ferrous sulfide (FeS) within 4–6 weeks (Fig. 2A; results for siderite not shown). Light microscopy showed a close association/attachment of the cells to the mineral particles. However, none of the three strains was able to oxidize vivianite (Fe<sub>3</sub>(PO<sub>4</sub>)<sub>2</sub>), magnetite (Fe<sub>3</sub>O<sub>4</sub>) or pyrite (FeS<sub>2</sub>) within 8 weeks. Interestingly, in contrast to experiments with siderite where all Fe(II) was oxidized, the bacteria did not oxidize the FeS to completion. After 4–6 weeks ~20% Fe(II) remained and no further oxidation was observed. When siderite was oxidized by the bacteria, the color of the precipitates turned greenish after some days before turning into an orange-brown color, likely indicating the presence of a mixed-valent Fe(II)/Fe(III) intermediate carbonate green rust precipitate (Onanguema et al., 2002).

### 3.2. Concentrations of Dissolved Fe(II) and Fe(III)

Following the addition of ferrous sulfide and siderite to the medium, significant concentrations of Fe(II) in solution were present after only 24 h (~40  $\mu$ M and ~250  $\mu$ M, respectively; Table 1); following the addition of vivianite, pyrite or magnetite, however, no dissolved Fe(II) could be detected with the ferrozine assay even after 4 weeks. These results reflect the

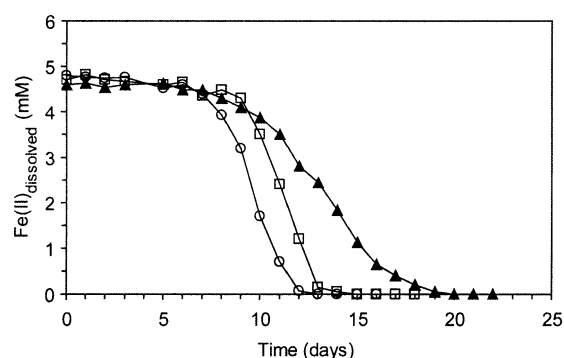


Fig. 1. Representative graphs for Fe(II)-oxidation in medium containing ~4.7 mM dissolved Fe(II) by anoxygenic photoautotrophic bacteria: *Rhodobacter ferrooxidans* strain SW2 (▲), *Chlorobium ferrooxidans* strain KoFox (□), and the *Thiodictyon* sp. strain F4 (○).

Table 1. Calculated and measured concentrations of dissolved ferrous iron in the presence of various iron(II) minerals.

Mineral	Formula		Log $K_{SP}$	Dissolved Fe(II) (calculated) [ $\mu\text{M}$ ] <sup>a</sup>	Dissolved Fe(II) (measured) [ $\mu\text{M}$ ] <sup>b</sup>
Siderite	$\text{FeCO}_3$	$\text{FeCO}_3(\text{s}) \rightleftharpoons \text{Fe}^{2+} + \text{CO}_3^{2-}$	-10.7 <sup>c</sup>	3	250
Vivianite	$\text{Fe}_3(\text{PO}_4)_2 \cdot 8\text{H}_2\text{O}$	$\text{Fe}_3(\text{PO}_4)_2 \cdot 8\text{H}_2\text{O} (\text{s}) \rightleftharpoons 3\text{Fe}^{2+} + 2\text{PO}_4^{3-} + 8\text{H}_2\text{O}$	-36.0 <sup>c</sup>	1.1	b.d.
FeS (precip) <sup>d</sup>	FeS	$\text{H}^+ + \text{FeS} \rightleftharpoons \text{Fe}^{2+} + \text{HS}^-$	-3.0 <sup>c</sup>	10	40
Pyrite	$\text{FeS}_2$	$\text{FeS}_2 \rightleftharpoons \text{FeS} (\text{Pyrrhotite}) + \text{S}^0$	-10.4 <sup>c</sup>	0.001	b.d.
Magnetite	$\text{Fe}_3\text{O}_4$	$8\text{H}^+ + \text{Fe}_3\text{O}_4 \rightleftharpoons 4\text{H}_2\text{O} + \text{Fe}^{2+} + 2\text{Fe}^{3+}$	+3.4 <sup>e</sup>	$2.9 \times 10^{-12}$	b.d.

<sup>a</sup> Calculated from the solubility constants  $K_{SP}$  and the respective ion speciation and concentrations in the medium (determined with MINEQL).

<sup>b</sup> Measured in medium 24 h after addition of the mineral.

<sup>c</sup> From Morel and Hering (1993).

<sup>d</sup> The value for an undefined ferrous sulfide precipitate was chosen. The  $K_{SP}$  values for the more defined FeS minerals Mackinawite (-3.6) and Pyrrhotite (-5.1) are slightly more negative leading to slightly smaller theoretical  $\text{Fe}^{2+}$ -concentrations.

<sup>e</sup> From MINEQL database.

b.d.: below detection limit.

relative equilibrium solubilities calculated for these different minerals in the medium used (Table 1).

When medium containing ferrous sulfide was inoculated with the three strains of Fe(II)-oxidizing bacteria, the concentrations of dissolved Fe(II) dropped to values that were no longer detectable when microbial Fe(II) oxidation began (Fig. 2B). In the uninoculated control, the dissolved Fe(II) concentration remained almost constant throughout the duration of the experiment. When siderite was added to the medium, the concentration of dissolved Fe(II) measured after 24 h was significantly higher than the predicted equilibrium concentration (Table 1) probably due to its relatively high surface area. In inoculated cultures, the dissolved Fe(II) concentration dropped to non-detectable values only when oxidation was nearly complete at the end of 6 weeks.

No dissolved ferric iron (Fe(III)) could be detected in any of the experiments.

### 3.3. X-ray Analysis of Fe(II)-Oxidation Products

To characterize the Fe(III)-precipitates produced as a consequence of photoautotrophic Fe(II)-oxidation and to follow the chemical transformations of these precipitates over time, bacterial culture suspensions were sampled at different time points and the minerals were investigated by X-ray analysis. The absence of distinct signals in the spectra of precipitates obtained from oxidation of dissolved Fe(II) by *R. ferroxidans* strain SW2 show that initially a poorly crystalline or even amorphous Fe(III)-phase is formed (Fig. 3). The spectrum of this early precipitate resembles the reference spectrum obtained for synthetic ferrihydrite. With aging, more crystalline phases could be observed. A comparison with spectra of synthetic goethite and the X-ray analysis database shows the presence of goethite and lepidocrocite in the older precipitates (Fig. 3). Precipitates produced from the oxidation of dissolved Fe(II) by KoFox and F4 showed similar spectra and temporal changes (results not shown).

Solids collected after 2 and 5 weeks of microbial oxidation of ferrous sulfide by strains SW2, F4, and KoFox showed no distinct signals of crystalline phases except for signals of remaining ferrous sulfide (Fig. 3). Apart from the signals belonging to ferrous sulfide, the spectra resembled those obtained for the poorly crystalline phases produced initially by the bacteria when oxidizing dissolved Fe(II). In these cultures, no temporal mineral evolution was observed with XRD.

### 3.4. Electron Microscopy

Biologic precipitation and subsequent chemical transformation of Fe(III)-minerals were also followed by electron microscopy. Scanning electron micrographs of 5-d old cultures of *R. ferroxidans* strain SW2 grown on dissolved Fe(II) showed that initially aggregates of 10–20  $\mu\text{m}$  size consisting of smaller aggregates of 1–3  $\mu\text{m}$  size were formed (Fig. 4A). These smaller aggregates consisted of particles that had a size of hundreds of nm and showed various shapes, e.g., needles and plates, in addition to irregular shapes (Fig. 4B,C). Generally,

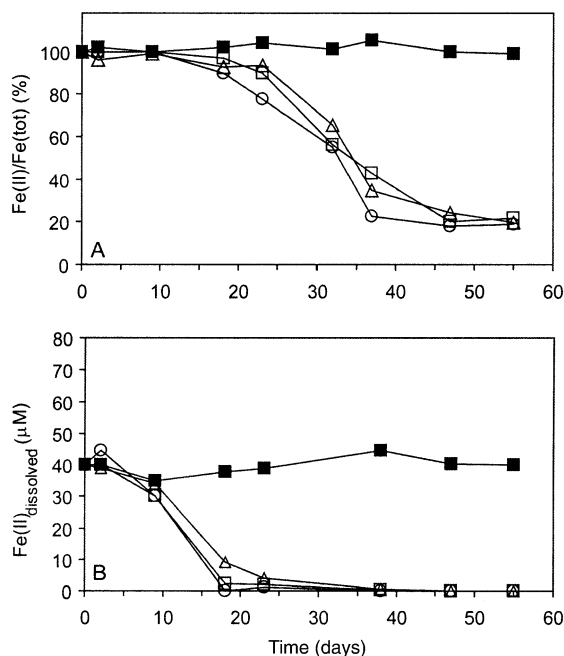


Fig. 2. Photoautotrophic oxidation of Fe(II) provided as ferrous sulfide. (A) Total Fe(II) (shown as relative amount of the total iron) and (B) concentrations of dissolved Fe(II) present in cultures of SW2 ( $\square$ ), KoFox ( $\triangle$ ), F4 ( $\circ$ ), compared to an uninoculated control ( $\blacksquare$ ).



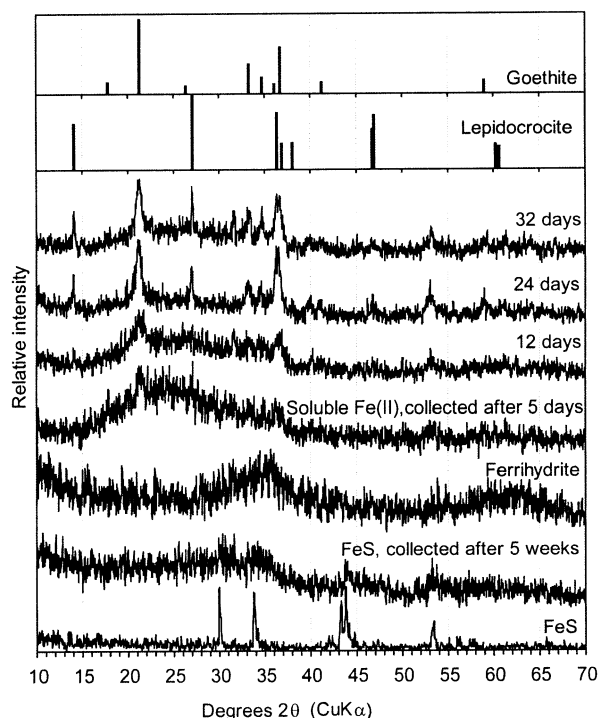


Fig. 3. X-ray diffractograms for precipitates collected at different time points from SW2 cultures oxidizing FeS or dissolved Fe(II). For comparison, a diffractogram of the FeS starting material, of synthetic poorly crystalline ferric hydroxide, and reference data from the International Centre for Diffraction Data (ICDD) are included.

the fresh precipitates appear poorly ordered. EDS analysis revealed that the precipitates consisted of iron and oxygen (see EDS-insert in Fig. 4A; non-labeled signals are due to background Cu, C and Si in the support grid).

Precipitates collected 2 weeks after inoculation showed principal aggregates (10–20  $\mu\text{m}$ ) that consisted of smaller aggregates ( $\sim 1 \mu\text{m}$ ) (Fig. 4D). However, compared to the fresh precipitates, the smaller aggregates consisted of more regular shaped particles with a size of several hundreds of nm (Fig. 4E). This was even more pronounced in 4 week old cultures, where many particles showed regular flower-like and star-like structures (Fig. 4F). EDS analysis again confirmed the presence of iron and oxygen.

Scanning electron micrographs of the precipitates produced by the two other strains KoFox and F4 under comparable conditions were similar to the precipitates produced by SW2 (images not shown).

Scanning electron micrographs of precipitates collected after 5 weeks of ferrous sulfide oxidation by SW2 (Fig. 4G,H) and by KoFox and F4 (images not shown) showed globular-shaped particles of several hundreds of nm size. EDS analysis of the globules (see insert in Fig. 4G) showed intense signals for Fe, O and P suggesting, together with the XRD results, that the globules consist of non-crystalline ferric (hydroxy)phosphates.

Transmission electron microscopy was used to investigate the microbe-mineral associations in SW2 cultures (grown on dissolved Fe(II)). Images were taken from cultures after 5 d, 6 weeks and 3 months incubation. After 5 d, free precipitates

were present as well as precipitates that were closely associated with the cells covering their exterior (Fig. 5A,B). These precipitates were identified as iron (hydr)oxides by EDS. The precipitates were found more or less homogeneously distributed around the cells; no areas with a significant enrichment of precipitates could be identified. Not all cells in a culture were covered by minerals, however. Even after 6 weeks or 3 months, many precipitate-free cells could be found (see Fig. 5C). We estimate that about 40–50% of the cells were precipitate-free in the older cultures, whereas only 10–20% were precipitate-free in the 5-d old cultures.

The thin sections prepared from a 3 month-old SW2 culture (Fig. 5C) also clearly revealed the more crystalline mineral particles that we observed with XRD and SEM.

### 3.5. Analysis of Culture Supernatants

To explore the possibility that Fe(III)-binding chelators were present in our cultures, culture supernatants and uninoculated controls were analyzed with ion chromatography (IC) and (high-pressure) liquid chromatography (HPLC and LC). The sample pH was increased before the analysis to precipitate the Fe(III) completely and to be sure that any ligands present were

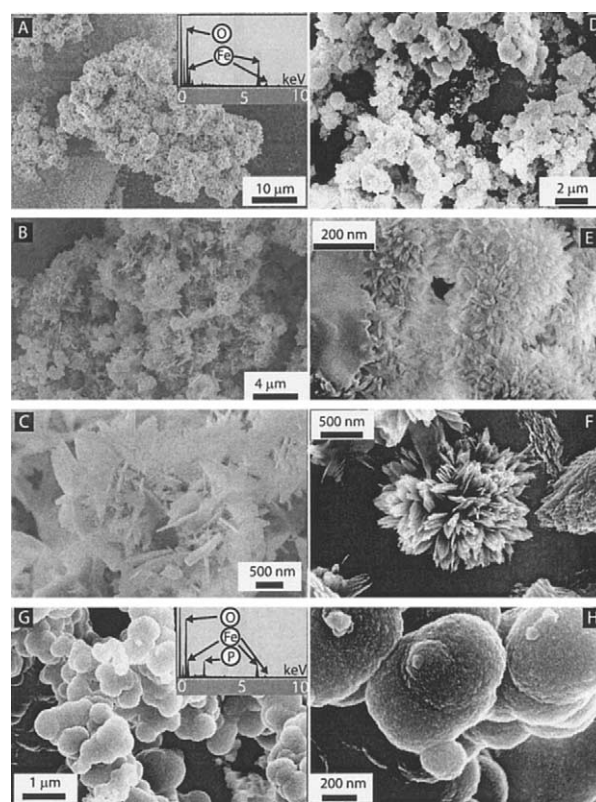


Fig. 4. Scanning electron micrographs of Fe(III)-precipitates produced by photoautotrophic Fe(II)-oxidizing bacteria and typical EDS-spectra obtained for the precipitates. (A–C) Fe(III)-precipitates produced within the first 5 d of oxidation of dissolved Fe(II) by SW2. (D–E) Precipitates collected after 2 weeks and (F) after 4 weeks illustrating the transformation to more crystalline and regular shaped particles. (G,H) Fe(III)-precipitates produced by SW2 when oxidizing ferrous sulfide (FeS). Samples were collected after 5 weeks.

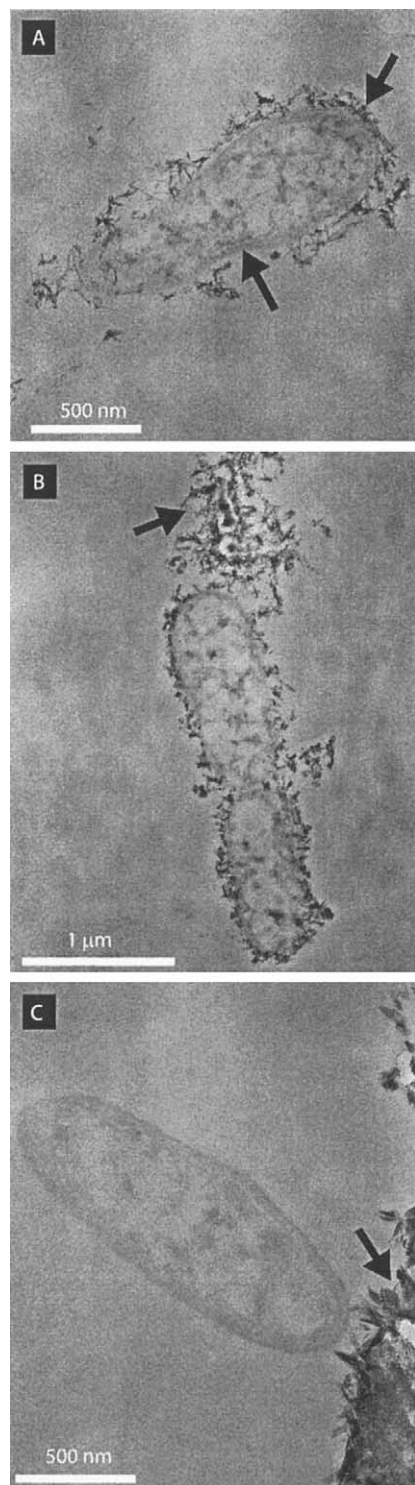


Fig. 5. Transmission electron micrographs of SW2 cultures at different time points during the oxidation of dissolved Fe(II): (A,B) Stained thin sections of a sample collected after 5 d. (C) Stained thin section of a sample collected after 3 months. The arrows indicate free and attached Fe(III)-particles (A,B), uncovered parts of the cell (A), or crystalline Fe(III)-precipitates (C).

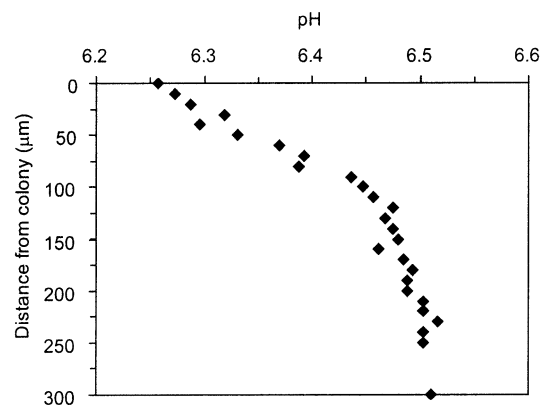


Fig. 6. Representative microelectrode measurements of the pH-microenvironment around a colony ( $\sim 300 \mu\text{m}$  diameter) of SW2 growing in medium solidified with 1% agar.

released from Fe(III). Analysis of SW2 culture supernatants (grown with dissolved Fe(II) or with FeS) showed no significant concentration of commonly excreted carboxylic and dicarboxylic acids (oxalate, oxalacetate, citrate, tartaric acid,  $\alpha$ -ketoglutarate, maleic acid, malate, pyruvate, lactate, succinate, formate, glutarate, acetate, fumarate or propionate).

However, in a few SW2, KoFox, and F4 culture supernatants, we could detect a compound that eluted at the retention time of citrate (chromatogram not shown) at a concentration of 30–1000 nM. LC-MS confirmed the compound as citrate. We were unable to identify specific conditions that induced the presence of this peak; its appearance seemed random. In addition to the citrate-peak, culture supernatants of F4 and KoFox analyzed with IC and (HP)LC reproducibly showed at least one other distinct peak that was not present in the uninoculated medium. This compound was always present in the cultures and its abundance did not correlate with their age. The compound did not co-elute with any of the carboxylic acids mentioned above. LC-MS analysis showed that this compound has a mass of 270, but its structure is currently unknown. Assuming this compound has a similar extinction coefficient to that of citrate, we estimate it was present at high nanomolar concentrations.

Testing of the culture supernatant with the CAS assay revealed that strong Fe(III)-chelators were not present.

### 3.6. Microelectrode Measurements

According to the metabolism of the photoautotrophic Fe(II)-oxidizing bacteria, protons should be produced, possibly acidifying the microenvironment around a cell or an association of cells. Microelectrode measurements of the pH around colonies of SW2 grown in solidified agar were used to test this prediction. As expected, we found that the pH in the microenvironment of the colonies (several hundred  $\mu\text{m}$ ) was slightly more acidic than the pH in the background agar (Fig. 6). The pH decrease observed is not as dramatic as expected due to the oxidation of 4–6 mM Fe(II), probably due to the buffer used in the medium and thus the consumption of most of the protons produced. Nevertheless, the results of the microelectrode measurements obtained even in buffered agar suggest that the

metabolism of photoautotrophic Fe(II)-oxidizing bacteria can lead to an acidification of their microenvironment.

#### 4. DISCUSSION

Motivated by a desire to better interpret the Fe isotope fractionation produced by photoautotrophic Fe(II)-oxidizing bacteria (Croal et al., 2004), we undertook the present study to identify the Fe(II) substrates that can be oxidized by these organisms and to analyze their mineral products. Specifically, we sought to address the question of whether free organic ligands are involved in the binding of Fe(II) and/or the release of Fe(III).

##### 4.1. Oxidation of Dissolved Fe(II)

Oxidation of Fe(II) by the photoautotrophic Fe(II)-oxidizing bacteria, *Rhodobacter ferrooxidans* strain SW2, *Chlorobium ferrooxidans* strain KoFox, and *Thiodictyon* sp. strain F4, appears to be similar with respect to the substrate used. In all cases, the bacteria could only grow and oxidize Fe(II) if dissolved Fe(II) was present in the medium. The only minerals that were sufficiently soluble were siderite and ferrous sulfide. We found no evidence for active dissolution of less soluble Fe(II)-minerals by microbially produced Fe(II)-solubilizing ligands. Similar trends were seen in a study performed with Fe(II)-oxidizing nitrate-reducing bacteria from the marine environment (Schippers and Joergensen, 2002). These bacteria were only able to oxidize Fe(II) provided as ferrous sulfide, whereas when given pyrite (which is relatively insoluble), no oxidation was observed. Further evidence in support of this comes from a study of two microaerophilic oxygen-dependent Fe(II)-oxidizing groundwater-enrichment cultures that could grow only on siderite and ferrous sulfide (Emerson and Moyer, 1997). Together, these observations support the conclusion that mineral solubility controls which Fe(II) substrates can sustain anaerobic microbial Fe(II)-oxidation. The pH dependence of mineral solubility, in turn, may explain why Fe(II)-oxidizing photoautotrophs have such a low and narrow pH optimum (Ehrenreich and Widdel, 1994; Heising et al., 1999).

Although the bacteria do not appear to actively solubilize Fe(II)-minerals through the excretion of organic ligands, their metabolism may nonetheless enhance dissolution through acidification of the local environment (Eqn. 1). For example, acidification of the microenvironment around cells or cell aggregates (as observed in our microelectrode experiments) may provoke dissolution of ferrous sulfide (FeS) as described in the following equation (Schippers and Joergensen, 2002):



Similarly, the dissolution of siderite (FeCO<sub>3</sub>) may be catalyzed by microbial acidification of the local environment, because siderite dissolves faster at pH values <5.5 (Duckworth and Martin, 2004). Evidence in support of this comes from the fact that the FeCO<sub>3</sub> dissolution rates measured in the absence of O<sub>2</sub> at pH values between 5 and 8 (Pokrovsky and Schott, 2002; Duckworth and Martin, in press) are 2–5 times lower than the dissolution rate necessary to account for the oxidation of FeCO<sub>3</sub> or FeS that occurred in our study. The higher dissolution rates in our bacterial cultures could be caused by the

described pH effect; however, it is also possible that the high ionic strength of our medium may have influenced dissolution by controlling the Fe(II)-mineral surface properties.

##### 4.2. Mineral Precipitation and Evolution

The first solids that appeared in our cultures resemble the poorly crystalline Fe(III) precipitates described for minerals produced by microaerophilic oxygen-dependent Fe(II)-oxidizing bacteria (Emerson and Moyer, 1997). Because the oxidation of Fe(II) produces Fe(III), which is expected to form Fe(III)(hydr)oxides at circumneutral pH (Schwertmann and Cornell, 2000), this is not surprising. Whereas poorly crystalline phases in dry form are stable for years, in aqueous solution they transform to goethite, hematite and lepidocrocite depending on the pH and solution chemistry (Schwertmann and Cornell, 2000); this is exactly what we observed in our experiments. Because transformation of poorly crystalline Fe(III) to goethite or lepidocrocite requires atomic reorganization (from a trigonal crystal system to an orthorhombic crystal system), dissolution and re-precipitation are necessary (Schwertmann and Cornell, 2000). This process is known to be catalyzed by reducing agents such as cysteine or Fe(II) (Schwertmann and Cornell, 2000). The relatively rapid transformation of the initial precipitates into more crystalline phases in our cultures (compared to abiotic systems in the absence of reducing agents) was likely stimulated by residual Fe(II) or by the bacteria. There are two ways that bacteria could have stimulated transformation: (1) through acidification of the local environment followed by an acid-catalyzed dissolution of Fe(III)-minerals or (2) by reduction of Fe(III). The presence of reducing agents or Fe(II) in combination with surface bridging ligands are known to stimulate reductive dissolution of poorly crystalline Fe(III)-oxides and subsequent re-precipitation of more highly ordered phases (Cornell et al., 1989; Cornell et al., 1991; Cornell and Schwertmann 1996). Notably, we observed a modest amount of Fe(III) reduction in cultures of SW2 incubated in the dark after addition of acetate or hydrogen in the presence of poorly crystalline Fe(III) (hydr)oxide (not shown); a similar reduction has been reported for *Rhodobacter capsulatus*, a close relative of SW2 (Dobbin et al., 1996) and for *Chlorobium ferrooxidans* (Heising et al., 1999). As bacterial cultures age, cell lysis typically occurs and liberates organic compounds that can drive the metabolism of the remaining non-lysed cells (Zinser and Kolter, 1999). Therefore it is probable that sufficient organic matter would have been present in our cultures to drive Fe(III) reduction.

##### 4.3. Microbe/Mineral Interactions

Although we do not yet know where enzymatic oxidation of Fe(II) to Fe(III) occurs within the cell (e.g., does it occur on the outer membrane, oriented away from the cell, or in an intracellular compartment?), we do know that the Fe(III) mineral products only occur outside the cell. Assuming Fe(III) is released as a cation, it has the potential to sorb onto negatively charged cell surfaces (Schultze-Lam et al., 1996; Konhauser, 1998). This raises the question of how the cell avoids encrustation by its own metabolic products. A lower pH around the cells as a consequence of metabolism could prevent precipita-



tion until the Fe(III) diffuses away from the cell and reaches a less acidic environment. Previously, it has been suggested that organic iron-chelating molecules may be involved in Fe(III)-release by Fe(II)-oxidizing phototrophs (Heising and Schink, 1998; Straub et al., 2001), and precipitation at a distance has also been invoked in the context of neutrophilic oxygen-dependent Fe(II)-oxidation (Sobolev and Roden, 2001).

Is there any evidence that free organic ligands facilitate precipitation at a distance? While we were able to detect nanomolar concentrations of citrate and other organic compounds in our cultures, due to the energetic requirement for their synthesis, the random nature of their appearance, and the fact that they did not appear to track with the growth phase, it is questionable whether they play a significant role in helping the cell avoid encrustation. Furthermore, we were unable to detect the presence of any strong Fe(III)-chelators (e.g., siderophores). This was expected given that siderophore production is known to be repressed when dissolved Fe concentrations exceed several micromolar (Earhart, 1996), and because the energetic costs of producing Fe(III)-specific ligands seem too high to make biologic sense when Fe is being used for energy generation rather than assimilation. Based on our data, and assuming that Fe(II) oxidation takes place on the cell surface as suggested by Ehrenreich and Widdel (1994), the most likely scenario for the liberation of Fe(III) from the cell is its release in a dissolved form either as an inorganic aqueous complex and/or as a colloidal aggregate. Mineral nucleation would then occur once the aggregates reach a certain critical size (von Gunten and Schneider, 1991).

The interactions of the Fe(III) mineral particles with the cells in our experiments (especially early in the incubation period) are highly reminiscent of those described for the sorption of various iron minerals to the cell wall of *Shewanella putrefaciens*. This can be explained by the fact that negatively-charged cell surfaces are known to electrostatically attract positively charged Fe(III)-aggregates. Rarely do we observe a continuous mineral deposit around the cell; rather, precipitates clump together, leaving large areas of the cell wall exposed. The patchiness of the precipitate cover may reflect heterogeneous distribution of charge on the cell surface (Sokolov et al., 2001), or it simply could be due to stochastic nucleation and steric limitation of further mineral development and/or adsorption in a given area. Interestingly, significantly more cells were precipitate-free in aged cultures than in fresh cultures. Whether this is a developmentally-regulated process, however, requires testing in future studies.

## 5. CONCLUSIONS

Diverse photoautotrophic bacteria can use Fe(II) as an electron donor for anoxygenic photosynthesis, but only appear to oxidize Fe(II) in its dissolved form. Poorly soluble Fe(II) minerals such as magnetite, pyrite and vivianite are not oxidized by these organisms, whereas the more soluble siderite and ferrous sulfide minerals are. This suggests that free Fe(II)-binding organic ligands are not released. Fe(II) is oxidized and appears to be released as a dissolved inorganic Fe(III) species that precipitates at a distance to the cell as poorly crystalline Fe(III) (hydr)oxide. These minerals transform over time into the more crystalline minerals goethite and lepidocrocite.

What bearing do our results have for the interpretation of Fe isotopic data obtained for this class of bacteria that show an enrichment of heavy Fe atoms in the Fe(III) mineral products relative to the Fe(II) substrates (Croal et al., 2004)? As summarized in Fig. 7, there are a number of steps that may affect the overall measured Fe isotope fractionation between the dissolved Fe(II) substrate and the Fe(III) mineral product. First, isotopic fractionation might occur during binding of Fe(II) from the medium to a receptor ligand on or in the cell (label 1, Fig. 7). Fractionation might also occur in a second step, during oxidation of the biologically bound Fe(II) to Fe(III) (label 2, Fig. 7). Third, isotopic exchange between free or cell-associated Fe(II) and Fe(III) might fractionate Fe (label 3, Fig. 7), as well as subsequent rapid (but not quantitative) precipitation of Fe(III) (hydr)oxide (label 4, Fig. 7). Fifth, adsorption of Fe(II) onto Fe(III) (hydr)oxide and/or cell surfaces (label 5, Fig. 7) might contribute. Finally, isotope fractionation might occur through back exchange between the mineral product and the dissolved iron species (label 6, Fig. 7). As discussed in detail in Croal et al. (2004), the most likely mechanisms that explain the observed fractionation are 1) an equilibrium effect produced by free or cell-associated biologic ligands (label 3, Fig. 7), or 2) a kinetic effect produced by precipitation of Fe(III) (hydr)oxide (label 4, Fig. 7) overlaid upon equilibrium exchange between Fe(II) and Fe(III) species.

The results of this study appear to rule out equilibrium exchange between free biologic ligands as an explanation for the observed fractionation: Fe(II)-binding organic ligands are not involved in Fe(II) mineral dissolution, and free Fe(III)-binding organic ligands are present only sporadically and when present, only at nanomolar concentrations. It is still possible, however, that cell-associated organic ligands contribute to establishing an equilibrium Fe isotope fractionation. Nevertheless, our results cause us to favor an abiotic explanation for the observed fractionation at this time given that we can explain the release of dissolved Fe(III) and subsequent nucleation/precip-

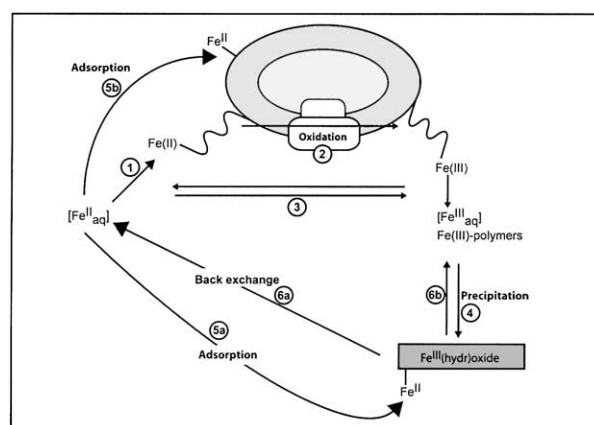


Fig. 7. Model for Fe(II)-oxidation by anoxygenic photoautotrophic bacteria. The numbers in circles indicate various processes that could lead to an iron isotope fractionation. (1) Fe(II)-binding by the cell, (2) microbial oxidation of Fe(II) to Fe(III) and subsequent release of Fe(III), (3) isotopic exchange between free or cell-associated Fe(II) and Fe(III) species, (4) precipitation of Fe(III)(hydr)oxides, (5a,b) adsorption of Fe(II) onto the Fe(III)(hydr)oxide or cell surface, respectively, and (6a,b) isotopic back-exchange between Fe(III)(hydr)oxide and dissolved Fe(II)- or Fe(III)-species.



itation of Fe(III) minerals by the low pH microenvironment surrounding metabolically active cells. Future experiments aimed at identifying specific cell-associated Fe(II) binding and oxidizing biomolecules and quantifying the kinetic fractionations produced by poorly crystalline Fe(III) (hydr)oxide precipitation are needed to resolve this issue.

*Acknowledgments*—We thank B. Schink and F. Widdel for supplying the strains used in this study, C. Ma for assistance with the XRD and SEM, R. Mielke for taking the TEMs, N. Dalleska for assistance with the LC-MS and IC, and Laura Croal and Mariu Hernandez for many stimulating discussions and helpful comments. This work was supported by a post doctoral fellowship to A.K. from the German Research Foundation (Deutsche Forschungsgemeinschaft) and by grants to D.K.N. from the Packard Foundation. We would also like to thank anonymous reviewers for their constructive comments and suggestions.

*Associate editor:* L. G. Benning

## REFERENCES

- Baker B. J. and Banfield J. F. (2003) Microbial communities in acid mine drainage. *FEMS Microbiol. Ecol.* **44**, 139–152.
- Beard B. L., Johnson C. M., Cox L., Sun H., Neelson K. H., and Aguilar C. (1999) Iron isotope biosignatures. *Science* **285**, 1889–1892.
- Benz M., Brune A., and Schink B. (1998) Anaerobic and aerobic oxidation of ferrous iron at neutral pH by chemoheterotrophic nitrate-reducing bacteria. *Arch. Microbiol.* **169**, 159–165.
- Beukes N. J. and Klein C. (1992) Models for iron-formation deposition. In *The Proterozoic Biosphere* (eds. J. W. Schopf and C. Klein). Cambridge University Press, Cambridge.
- Blake R. C., Shute E. A., Greenwood M. M., Spencer G. H., and Ingledew W. J. (1993) Enzymes of aerobic respiration on iron. *FEMS Microbiol. Rev.* **11**, 9–18.
- Braterman P. S., Carins-Smith A. G., and Sloper R. W. (1983) Photo-oxidation of hydrated Fe<sup>2+</sup>- significance for banded iron formations. *Nature* **303**, 163–164.
- Bullen T. D., White A. F., Childs C. W., Vivit D. V., and Schulz M. S. (2001) Demonstration of significant abiotic iron isotope fractionation in nature. *Geology* **29**, 699–702.
- Cairns-Smith A. G. (1978) Precambrian solution photochemistry, inverse segregation, and banded iron formation. *Nature* **276**, 807–808.
- Cornell R. M. and Schwertmann U. (1996) *The Iron Oxides: Structure, Properties, Reactions, Occurrences and Uses*. VCH, Weinheim.
- Cornell R. M., Schneider W., and Giovanoli R. (1989) The transformation of ferrihydrite into lepidocrocite. *Clay Minerals* **24**, 549–553.
- Cornell R. M., Schneider W., and Giovanoli R. (1991) Preparation and characterization of colloidal alpha-FeOOH with a narrow size distribution. *J. Chem. Soc., Faraday Trans.* **87**, 869–873.
- Croal L. R., Johnson C. M., Beard B. L., and Newman D. K. (2004) Iron isotope fractionation by anoxygenic Fe(II)-oxidizing phototrophs. *Geochim. Cosmochim. Acta* in press.
- Dobbin P. S., Warren L. H., Cook N. J., McEwan A. G., Powell A. K., and Richardson D. J. (1996) Dissimilatory iron(III) reduction by *Rhodobacter capsulatus*. *Microbiology* **142**, 765–774.
- Duckworth O. W. and Martin S. T. (2004) Role of molecular oxygen in the dissolution of siderite and rhodochrosite. *Geochim. Cosmochim. Acta* **68**, 607–621.
- Earhart C. F. (1996) Uptake and metabolism of iron and molybdenum. In *Escherichia coli and Salmonella* (ed. F. C. Neidhart), p. 1083. ASM Press.
- Edwards K. J., Bond P. L., Gihring T. M., and Banfield J. F. (2000) An archaeal iron-oxidizing extreme acidophile important in acid mine drainage. *Science* **287**, 1796–1799.
- Edwards K. J., McCollom T. M., Konishi H., and Buseck P. R. (2003) Seafloor bioalteration of sulfide minerals: Results from *in situ* incubation studies. *Geochim. Cosmochim. Acta* **67**, 2843–2856.
- Ehrenreich A. and Widdel F. (1994) Anaerobic oxidation of ferrous iron by purple bacteria, a new type of phototrophic metabolism. *Appl. Environ. Microbiol.* **60**, 4517–4526.
- Emerson D. and Moyer C. (1997) Isolation and characterization of novel iron-oxidizing bacteria that grow at circumneutral pH. *Appl. Environ. Microbiol.* **63**, 4784–4792.
- Francois L. M. (1986) Extensive deposition of banded iron formations was possible without photosynthesis. *Nature* **320**, 352–354.
- Glasauer S., Langley S., and Beveridge T. J. (2001) Sorption of Fe (hydr)oxides to the surface of *Shewanella putrefaciens*: Cell-bound fine-grained minerals are not always formed *de novo*. *Appl. Environ. Microbiol.* **67**, 5540–5550.
- Hartman H. (1984) The evolution of photosynthesis and microbial mats: A speculation on banded iron formations. In *Microbial Mats: Stromatolites* (ed. Y. Cohen, R. W. Castenholz, and H. O. Halvorson), pp. 451–453. Alan Liss, NY.
- Heising S. and Schink B. (1998) Phototrophic oxidation of ferrous iron by a *Rhodospirillum rubrum* strain. *Microbiology* **144**, 2263–2269.
- Heising S., Richter L., Ludwig W., and Schink B. (1999) *Chlorobium ferrooxidans* sp.nov., a phototrophic green sulfur bacterium that oxidizes ferrous iron in coculture with a *Geospirillum* sp. strain. *Arch. Microbiol.* **172**, 116–124.
- James H. L. and Sims P. K. (1973) Precambrian iron-formations in the world. *Econ. Geol.* **68**, 913–914.
- Johnson C. M., Beard B. L., Beukes N. J., Klein C., and O'Leary J. M. (2003) Ancient geochemical cycling in the Earth as inferred from Fe isotope studies of banded iron formations from the Transvaal Craton. *Contrib. Mineral. Petrol.* **144**, 523–547.
- Kasting J. F. (1993) Earth's early atmosphere. *Science* **259**, 920–926.
- Konhauser K. O. (1998) Diversity of bacterial iron mineralization. *Earth-Science Reviews* **43**, 91–121.
- Konhauser K. O., Hamade T., Raiswell R., Morris R. C., Ferris F. G., Southam G., and Canfield D. E. (2002) Could bacteria have formed the Precambrian banded iron formations? *Geology* **30**, 1079–1082.
- Morel F. M. M. and Hering J. G. (1993) *Principles and applications of aquatic chemistry*. Wiley, New York.
- Ona-Nguema G., Abdelmoula M., Jorand F., Benali O., Géhin A., Block J.-C., and Génin J.-M. R. (2002) Iron(II,III) hydroxycarbonate green rust formation and stabilization from lepidocrocite bioreduction. *Environ. Sci. Technol.* **36**, 16–20.
- Pokrovsky O. S. and Schott J. (2002) Surface chemistry and dissolution kinetics of divalent metal carbonates. *Environ. Sci. Technol.* **36**, 426–432.
- Schippers A. and Joergensen B. B. (2002) Biogeochemistry of pyrite and iron sulfide oxidation in marine sediments. *Geochim. Cosmochim. Acta* **66**, 85–92.
- Schultze-Lam S., Fortin D., Davis B. S., and Beveridge T. J. (1996) Mineralization of bacterial surfaces. *Chem. Geol.* **132**, 171–181.
- Schwertmann U. and Cornell R. M. (2000) *Iron Oxides in the Laboratory. Preparation and Characterization*. John Wiley & Sons, Weinheim, Germany.
- Schwyn B. and Neilands J. B. (1987) Universal chemical assay for the detection and determination of siderophores. *Anal. Biochem.* **160**, 47–56.
- Sobolev D. and Roden E. E. (2001) Suboxic deposition of ferric iron by bacteria in opposing gradients of Fe(II) and oxygen at circumneutral pH. *Appl. Environ. Microbiol.* **67**, 1328–1332.
- Sokolov I., Smith D. S., Henderson G. S., Gorby Y. A., and Ferris F. G. (2001) Cell surface electrochemical heterogeneity of the Fe(III)-reducing bacteria *Shewanella putrefaciens*. *Environ. Sci. Technol.* **35**, 341–347.
- Stookey L. L. (1970) Ferrozine - a new spectrophotometric reagent for iron. *Anal. Chem.* **42**, 779–781.
- Straub K. L. and Buchholz-Cleven B. E. (1998) Enumeration and detection of anaerobic ferrous iron-oxidizing, nitrate-reducing bac-

- teria from diverse European sediments. *Appl. Environ. Microbiol.* **64**, 4846–4856.
- Straub K. L., Benz M., and Schink B. (2001) Iron metabolism in anoxic environments at near neutral pH. *FEMS Microbiol. Rev.* **34**, 181–186.
- Stumm W. and Morgan J. J. (1996) *Aquatic Chemistry: Chemical Equilibria and Rates in Natural Waters* (ed. J. L. Schnoor and A. Zehnder), 3d ed., John Wiley & Sons, New York.
- Trendall A. F. and Morris R. C. (1983) *Iron-Formation: Facts & Problems*. Elsevier, Amsterdam, 1–558.
- von Gunten U. and Schneider W. (1991) Primary products of the oxygenation of iron(II) at an oxic-anoxic boundary: Nucleation, aggregation, and aging. *J. Coll. Interf. Sci.* **145**, 127–139.
- Widdel F., Schnell S., Heising S., Ehrenreich A., Assmus B., and Schink B. (1993) Ferrous iron oxidation by anoxygenic phototrophic bacteria. *Nature* **362**, 834–836.
- Zinser E. R. and Kolter R. (1999) Mutations enhancing amino acid catabolism confer a growth advantage in stationary phase. *J. Bacteriol.* **181**, 5800–5807.